ELSEVIER

International Journal of Mass Spectrometry 214 (2002) 365–374

International Journal of Mass Spectrometry

www.elsevier.com/locate/ijms

Absolute total and partial electron ionization cross sections of C_2F_6

R. Basner[a,*], M. Schmidt[a], E. Denisov[a], P. Lopata[b], K. Becker[b], H. Deutsch[c]

[a] *Institut für Niedertemperatur-Plasmaphysik, Ernst-Moritz-Arndt-Universität, Friedrich-Ludwig Jahn Strasse 29, D-17489 Greifswald, Germany*

[b] *Department of Physics and Engineering Physics, Stevens Institute of Technology, Hoboken, NJ 07030, USA*

[c] *Institut für Physik, Ernst-Moritz-Arndt-Universität, Domstr. 10a, D-17489 Greifswald, Germany*

Received 16 November 2001; accepted 14 January 2002

Abstract

We measured absolute partial and total cross sections for the electron ionization of hexafluoroethane (C_2F_6) from threshold to 900 eV using a time-of-flight mass spectrometer (TOF-MS), which can be operated in a linear and in a reflection mode. Measurements were also made for tetrafluoromethane (CF_4), which is perhaps the most thoroughly investigated complex polyatomic molecule in terms of ionization cross sections, in an effort to demonstrate the reliable performance of our apparatus. Our measurements for both CF_4 and C_2F_6 are compared with other available experimental data and with calculated cross sections. (Int J Mass Spectrom 214 (2002) 365–374) © 2002 Elsevier Science B.V. All rights reserved.

Keywords: Tetrafluoromethane; Hexafluoroethane; Electron ionization; Cross sections; Plasma etching

1. Introduction

Simple fluorocarbon compounds such as CF_4, C_2F_6, and C_3F_8 are routinely used in the semiconductor industry as etching gases in various plasma-assisted material processing applications. In these applications, a quantitative knowledge of the interaction of these molecules with low-energy electrons of energies up to 100 eV is crucial (1) for the optimization of the performance parameters of a particular process, and (2) as input data for modeling codes. CF_4 is the most thoroughly investigated fluorocarbon molecule in terms of electron interactions [1]. Much less information is available regarding electron interactions with C_2F_6 [2] and C_3F_8 [3].

Here we report the results of measurements of the partial ionization cross sections of C_2F_6 for which few ionization data are available in the literature. Poll and Meichsner [4] measured the partial cross sections for ionization of C_2F_6 leading to the formation of selected ions ($C_2F_5^+$, CF_3^+, CF_2^+, and CF^+) up to an impact energy of 130 eV using a quadrupole mass spectrometer. However, the reliability of these first data are limited because already the CF_4 cross section data measured in the same experiments deviate noticeable from the recommended data [1] for the fragment ion CF^+ (at 70 eV: about 50%). Bibby and Carter [5] reported earlier ionization data, but only at a single electron energy of 35 eV. Their cross sections were much lower than the cross sections of Poll and Meichsner [4]. More recently, Jiao et al. [6] published results of measurements of partial ionization cross sections of

* Corresponding author. E-mail: basner@inp-greifswald.de

1387-3806/02/$20.00
PII S1387-3806(02)00541-9

C_2F_6 using Fourier transform mass spectrometry in the electron impact energy range from threshold up to 70 eV. They measured cross sections for the formation of the same four ions as reported in [4] and found higher partial cross sections for the CF^+ and $CF_2{}^+$ ions than Poll and Meichsner [4].

We measured a set of partial ionization cross section for C_2F_6 which include the fragment ions $C_2F_5{}^+$, $C_2F_4{}^+$, $CF_3{}^+$, $CF_2{}^+$, C_2F^+, CF^+, $C_2{}^+$, F^+, and C^+ for electron energies from threshold up to 900 eV. These measurements continue our ongoing study of ionization cross section measurements of molecules which are important for a microscopic understanding of the processes in low-temperature processing plasmas [7–14]. Some measurements were carried out using a modified high resolution double-focusing mass spectrometer (MCH 1310) with a Nier-type electron impact ion source [7–12], which result in reliable absolute ionization cross sections for ions that are formed with little, if any excess kinetic energy. However, our device (MCH 1310) has inherent limitations in cases where fragment ions are formed with a significant amount of excess kinetic energy. Therefore, we developed a time-of-flight mass spectrometer (TOF-MS) similar in design to the apparatus used by Bonham and co-workers [15] and Lindsay and co-workers [16]. Recently, our new apparatus was successfully used in the measurements of absolute partial electron-impact ionization cross sections of titanium tetrachloride [13] and of tetrafluorosilane [14].

In an effort to verify the reliable performance of our TOF-MS, we also measured absolute partial ionization cross sections for tetrafluoromethane (CF_4), which is perhaps the most thoroughly investigated complex polyatomic molecule, particularly in terms of partial ionization cross sections for fragment ions that are formed with excess kinetic energy [17–23]. Our results for CF_4 were found to be in good agreement with these "benchmark" data which agree with each other within their combined error margins (10–15%). Preliminary results of our C_2F_6 ionization cross section measurements have already been reported at a conference [24] and a comparison is also made with available calculated C_2F_6 ionization cross sections [2,25].

2. Experiment

The experimental apparatus and the procedure employed here to obtain absolute partial ionization cross sections have been described in detail in before [13,14]. Briefly, the TOF-MS is shown schematically in Fig. 1. It consists of two stainless-steel vacuum chambers evacuated separately by turbo-molecular pumps to a base pressure of 1×10^{-6} Pa. One chamber contains the electron impact ion source and the other chamber houses the ion drift tube and the ion detectors. The TOF-MS can be operated either in a linear mode using detector I or in a reflection mode using the reflector (grids: G_3, G_4, G_5 made from copper with 94% optical transmission) and detector II. Both detectors are micro-channel plate detectors (MCP, dual-plate chevron arrangement, Galileo Electro-Optics Corp.) of 40 mm diameter. In the present study, all measurements were performed with the TOF-MS operated in the linear mode to ensure complete ion transport from the ion source to the detector. The ion source chamber was filled with the target gas under study at pressures of about 1×10^{-4} Pa, which was measured with a spinning rotor viscosity gauge. Argon, which was used as reference gas, was always added to the ion source for calibration purposes. The ion efficiency curves (relative partial ionization cross sections) were measured simultaneously for Ar and CF_4 or C_2F_6 in a well-defined gas mixture in an effort to ensure identical operating conditions for the detection of the ions of each gas. The measured relative partial ionization cross sections were put on an absolute scale by normalization relative to the total Ar ionization cross section of 2.77×10^{-16} cm^2 at 70 eV [26]. Taking into account the uncertainties of ±7% in the Ar reference cross section [26], the statistical uncertainty in our pressure measurement of ±3%, and the counting statistics of ±5%, we assign an overall uncertainty of about ±15% to the absolute ionization cross sections reported here.

Typically, the electron gun was operated using electron pulses of 90 ns width at a repetition rate of 15 kHz. The electron beam has a diameter of about 0.6 mm in the interaction region and the amplitude of the

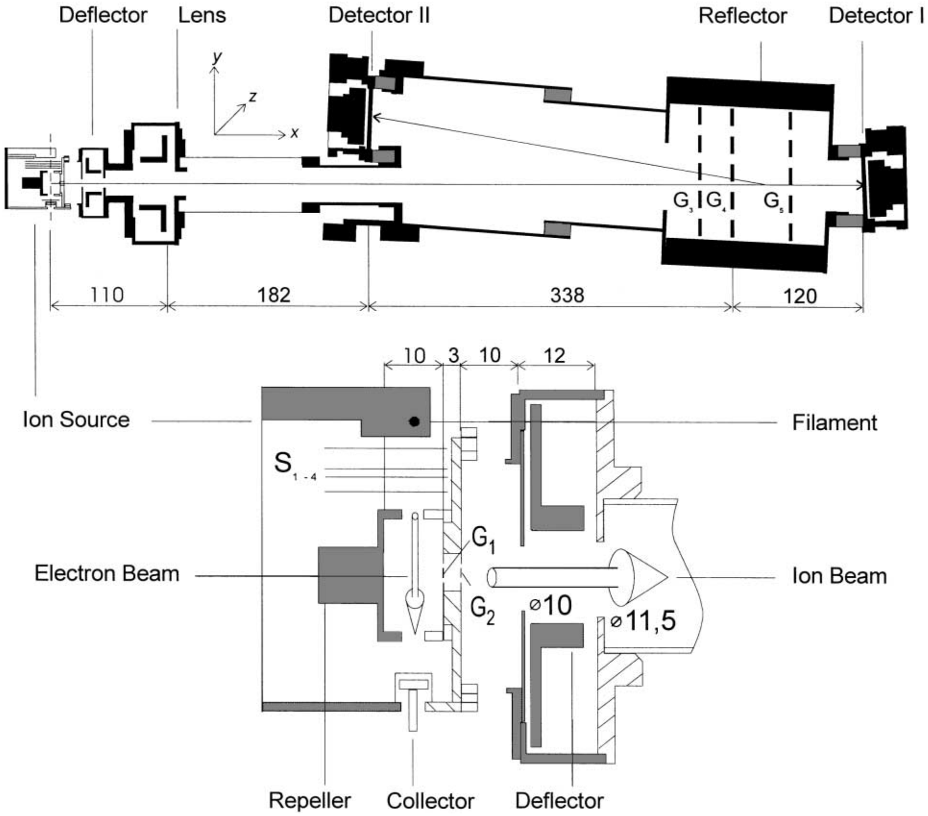

Fig. 1. Schematic diagram of the TOF-MS and an expanded view of the electron impact ion source used in the present study (all dimensions are in mm): electron beam (tungsten filament, 0 to −900 V); apertures: S_1 (0.5 mm × 4 mm, 22.4 V pre-acceleration), S_2/S_3 (0.5 mm × 4 mm, 22.4 or 70 V below the potential of the filament, pulsed), S_4 (0.4 mm × 0.4 mm, grounded); repeller (0 to ±3 kV); collision chamber exit aperture (6.5 mm × 6.5 mm, molybdenum grids (G_1, G_2): transmission 90%; grounded); flight tube entrance electrode (diameter 10 mm, 0 to ±3 kV); deflector (0 to ±500 V); Einzel lense (0 to ±13 kV); reflector (copper grids (G_3, G_4, G_5): transmission 94%); detectors I and II (Galileo, 40 mm diameter MCP, active area 12.5 cm^2).

electron pulse is in the range from 1–10 μA with an energy spread of about 0.5 eV (FWHM). The impact energy was varied from 5 to 900 eV and the electron beam is guided by a weak magnetic field (200 G). Extraction fields up to 3 kV/cm with a 10 ns rise time were employed to the repeller roughly 10 ns after the incident electron pulse passed through the ionization region. This extraction pulse accelerates the ions formed by electron impact towards the grounded ion source exit aperture. After passing through the exit aperture (grids: G_1, G_2 made from molybdenum with 90% optical transmission) the ions are accelerated by a −3 kV bias voltage applied to the entrance electrode of the flight tube. The ion deflector section consists of two pairs of electrodes for the deflection of the ions in the horizontal (z) and vertical (y) directions. The deflection plates in conjunction with the Einzel lens allow corrections of the ion trajectories. The first detector arrangement (detector I) is placed at the end of the flight tube. When the TOF-MS is operated in the reflection mode with much higher mass resolution ($m/\Delta m = 1500$ as compared to a mass resolution of about 50 in the linear mode for high extraction field), the three additional grids G_3, G_4, G_5 are employed to reverse the direction of the ions which are then detected by the second detector arrangement (detector II). The output from the MCP is preamplified and recorded with a 2 GHz multiscaler (FAST ComTec, Model 7886) using a time resolution of 500 ps. Our TOF-MS was operated in such a way that no more than one ion is created during each electron pulse. This results in low overall count rates and comparatively long data acquisition times, but ensures, on the other hand, that dead time corrections to the recorded signal rates are negligible. We further maintained operating conditions under which the ion count rate varied linearly with the gas pressure and the electron beam current.

Fragment ions resulting from the dissociative ionization of a molecule are often formed with excess kinetic energies, which can interfere with the complete extraction and transmission of the ions from the interaction region to the detector. Fragment ions of CF_4 are generally known to be formed with significant amounts of excess kinetic energies [17,23,27]. In our experiment, the excess kinetic energy causes the following effects:

(i) The ion source region, which is normally determined by the spatial dimensions of the electron beam, is enlarged because of the motion of the ions during the time interval between their formation and their extraction.
(ii) The divergence of the extracted "ion beam" is enlarged both spatially as well as temporally due to the variation in the spatial positions, momenta, and energies of the ions when the extraction pulse is applied.

Measurements of the ion extraction efficiency as a function of the delay time between the end of the electron pulse and the beginning of the extraction pulse to the repeller revealed constant ion currents for all fragment ions as long as the delay times were below 20 ns. This indicates that all ions from the extraction region of the ion source are transported to the detector under these conditions. Furthermore, extensive studies varying the voltages on the Einzel lens and on the horizontal and vertical deflection plates ensured that the diameter of the "ion beam" at the end of the flight tube is smaller than the diameter of the MCP (40 mm) for every fragment ion. We conclude that the experimental conditions necessary for 100% ion transmission of the ions from the ion source to the detector were established with the exception of ion loss at the grids G_1 and G_2.

Since our technique relies on measurements of ratios of ions, the detection efficiency of the MCP for the reference ion and the various product ions of the gas under study must be the same. A series of experiments was performed to measure the ion count rate of a constant incident ion flux as a function of the ion impact energy for given operating voltages of the MCP and threshold levels of the multiscaler. Increasing the ion energy and the operating voltage of the MCP while decreasing the threshold level of the multiscaler revealed a saturation value of the recorded ion count rate. The saturation for doubly charged ions at the same ion impact energy always occurred at a lower operating voltage of the MCP as expected. Optimum operating conditions were found for voltages of 2 kV across both channel plates with a voltage difference of 300 V between the last plate and the anode. A minimum threshold level of the multiscaler well above the noise level was selected in such a way that the ion count rate was saturated for all singly charged ions with ion impact energies higher than 3.2 keV (0.5 keV from the extraction and 2.7 keV from the acceleration) and for all doubly charged ions with twice the ion impact energies. We assume that the ion impact energy is high enough to guarantee a 100% counting efficiency for each ion hitting the front channel plate.

3. Results and discussion

3.1. Electron ionization of CF_4

We carried out a comprehensive study of the electron impact ionization of CF_4, for which careful partial ionization cross sections measurements have been carried out [19,23], in an effort to check the reliable performance of our apparatus. Our results for the partial

Table 1
Absolute partial (counting) and total (charge weighed) electron ionization cross sections for CF_4 as a function of electron energy

Electron energy (eV)	Ionization cross section (10^{-16} cm^2)							
	Ion							Total
	CF_3^+	CF_2^+	CF_3^{2+}	CF^+	CF_2^{2+}	F^+	C^+	
16	0.034							0.034
17	0.047							0.047
18	0.094							0.094
19	0.17							0.17
20	0.27							0.27
22	0.47	0.004						0.474
24	0.73	0.014						0.744
26	1.00	0.044						1.044
28	1.35	0.067						1.417
30	1.72	0.097		0.004				1.82
32	1.89	0.12		0.010				2.02
34	2.07	0.14		0.017				2.23
36	2.25	0.16		0.033		0.003	0.002	2.45
38	2.38	0.18		0.050		0.005	0.004	2.62
40	2.63	0.21		0.070		0.013	0.014	2.94
45	2.89	0.23	0.002	0.15	0.002	0.041	0.060	3.38
48	3.03	0.25	0.003	0.17	0.003	0.072	0.095	3.63
50	3.18	0.27	0.004	0.19	0.004	0.091	0.11	3.86
55	3.42	0.30	0.006	0.26	0.009	0.17	0.16	4.34
60	3.53	0.31	0.007	0.30	0.014	0.24	0.19	4.61
65	3.64	0.33	0.009	0.33	0.021	0.31	0.21	4.88
70	3.72	0.34	0.011	0.35	0.027	0.37	0.23	5.09
80	3.86	0.36	0.015	0.39	0.037	0.45	0.26	5.42
90	3.94	0.37	0.019	0.42	0.047	0.51	0.29	5.66
100	3.95	0.38	0.021	0.43	0.055	0.59	0.31	5.81
120	3.93	0.39	0.025	0.45	0.064	0.74	0.34	6.03
150	3.84	0.39	0.027	0.46	0.067	0.85	0.36	6.09
200	3.68	0.37	0.027	0.44	0.066	0.90	0.35	5.93
250	3.48	0.34	0.024	0.39	0.060	0.85	0.33	5.56
300	3.23	0.32	0.022	0.36	0.056	0.77	0.30	5.14
400	2.84	0.27	0.018	0.30	0.048	0.65	0.24	4.43
500	2.57	0.24	0.016	0.25	0.038	0.54	0.21	3.92
600	2.34	0.22	0.014	0.21	0.033	0.46	0.19	3.51
700	2.13	0.19	0.012	0.19	0.030	0.40	0.17	3.16
800	1.94	0.17	0.011	0.17	0.026	0.35	0.15	2.85
900	1.85	0.16	0.010	0.16	0.024	0.31	0.13	2.68

and total CF_4 ionization cross sections, which are summarized in Table 1 for impact energies up to 900 eV, are in excellent agreement with the cross sections reported by Bruce and Bonham [19] and by Poll et al. [23] in terms of the absolute cross section values and the cross section shape. One exception is the formation of F^+ fragment ions, where our absolute cross section exceeds the cross sections of [19,23] by about 20%. The demonstrated ability of our apparatus and experimental technique to reproduce the "benchmark" cross sections of [19,23] gives us confidence that we can measure reliable absolute partial cross sections for the dissociative ionization of polyatomic molecules at the ±15% level of accuracy even in cases where the fragment ions are produced by a significant amount of excess kinetic energy.

3.2. Electron ionization of C_2F_6

The ionization cross sections for the formation of all singly charged ions measured as part of this study for impact energies up to 900 eV are summarized in Tables 2 and 3, which also lists the total (single) C_2F_6 ionization cross section. No appreciable ion signals were detected that correspond to the formation of the singly charged parent ion $C_2F_6^+$ and the singly charged fragment ions $C_2F_3^+$ and $C_2F_2^+$ or the formation of any doubly charged ions. Fig. 2 shows the partial ionization cross section for the four most abundant fragment ions from threshold to 200 eV. CF_3^+ is the fragment ion with the largest partial ionization cross section with a maximum value of slightly less than $4 \times 10^{-16}\,cm^2$ at 80 eV followed by the $C_2F_5^+$ partial ionization cross section with roughly half the maximum value of the CF_3^+ cross section.

Table 2
Absolute partial electron ionization cross sections for the formation of $C_2F_5^+$, $C_2F_4^+$, CF_3^+, CF_2^+, and C_2F^+ fragment ions of C_2F_6 as a function of electron energy

Electron energy (eV)	Partial ionization cross section ($10^{-16}\,cm^2$)				
	$C_2F_5^+$	$C_2F_4^+$	CF_3^+	CF_2^+	C_2F^+
16			0.011		
17	0.025		0.063		
18	0.071		0.11		
19	0.13		0.18		
20	0.21		0.25		
22	0.38		0.49	0.0011	
24	0.54		0.80	0.0074	
26	0.69		1.05	0.016	
28	0.84		1.34	0.026	
30	0.97		1.56	0.046	
32	1.12	0.0012	1.74	0.070	
34	1.23	0.0019	1.91	0.098	
36	1.34	0.0025	2.06	0.12	
38	1.41	0.0030	2.20	0.16	
40	1.49	0.0035	2.33	0.19	
45	1.70	0.0045	2.70	0.30	0.0082
48	1.81	0.0049	2.91	0.35	0.010
50	1.91	0.0052	3.05	0.40	0.012
55	2.05	0.0056	3.26	0.48	0.016
60	2.13	0.0058	3.45	0.54	0.020
65	2.18	0.0060	3.58	0.61	0.023
70	2.23	0.0063	3.66	0.65	0.025
80	2.26	0.0066	3.77	0.75	0.031
90	2.27	0.0069	3.78	0.81	0.034
100	2.25	0.0071	3.74	0.84	0.036
120	2.18	0.0072	3.66	0.85	0.037
150	2.10	0.0069	3.54	0.84	0.035
200	2.06	0.0063	3.37	0.81	0.031
250	1.97	0.0056	3.19	0.74	0.028
300	1.87	0.0049	3.02	0.69	0.023
400	1.67	0.0039	2.70	0.59	0.018
500	1.50	0.0031	2.40	0.49	0.015
600	1.37	0.0028	2.13	0.43	0.013
700	1.25	0.0023	1.94	0.37	0.011
800	1.12	0.0019	1.77	0.33	0.009
900	1.04	0.0017	1.66	0.30	0.008

Table 3
Absolute partial electron ionization cross sections for the formation of CF^+, $C_2{}^+$, F^+, and C^+ fragment ions and total cross section of C_2F_6 as a function of electron energy

Electron energy (eV)	Partial ionization cross section (10^{-16} cm^2)				
	Ion				Total
	CF^+	$C_2{}^+$	F^+	C^+	
16					0.011
17					0.088
18					0.18
19					0.31
20					0.46
22	0.0024				0.87
24	0.0079				1.36
26	0.020				1.78
28	0.031				2.24
30	0.044				2.62
32	0.061				3.00
34	0.088				3.33
36	0.12				3.65
38	0.16				3.94
40	0.22				4.24
45	0.40		0.0038	0.0033	5.12
48	0.51		0.0065	0.0058	5.61
50	0.57		0.0092	0.0084	5.97
55	0.69		0.017	0.014	6.53
60	0.79		0.024	0.024	6.98
65	0.88	0.0018	0.034	0.036	7.35
70	0.95	0.0031	0.046	0.048	7.62
80	1.09	0.0050	0.078	0.079	8.07
90	1.19	0.0069	0.10	0.10	8.30
100	1.24	0.010	0.13	0.12	8.37
120	1.27	0.016	0.17	0.16	8.35
150	1.27	0.020	0.21	0.18	8.20
200	1.22	0.021	0.23	0.19	7.94
250	1.13	0.020	0.22	0.18	7.48
300	1.02	0.015	0.20	0.17	7.01
400	0.86	0.011	0.17	0.13	6.15
500	0.73	0.0076	0.14	0.11	5.40
600	0.61	0.0051	0.11	0.09	4.76
700	0.55	0.0035	0.09	0.07	4.29
800	0.48	0.0029	0.08	0.06	3.85
900	0.45	0.0023	0.07	0.06	3.59

Incidentally, the same partial ionization cross section ordering was also observed earlier for the electron impact ionization of the C_2F_5 free radical [28]. Other fragment ions that are formed with a maximum cross section of about 1×10^{-16} cm^2 are CF^+ and $CF_2{}^+$ which are also shown in Fig. 2. Cross sections for these four fragment ions were also reported in the earlier study of Poll and Meichsner [4] and in the recent paper of Jiao et al. [6]. The present cross sections are in plausible agreement with these previous results within their combined margin of error. The only exception is the energy range below 40 eV for CF^+ where our cross section data show a more gradual increase. In accordance with Jiao et al. [6], we find higher yields (by 25%) of $CF_2{}^+$ and CF^+ above 40 eV and similar shapes near threshold for $C_2F_5{}^+$

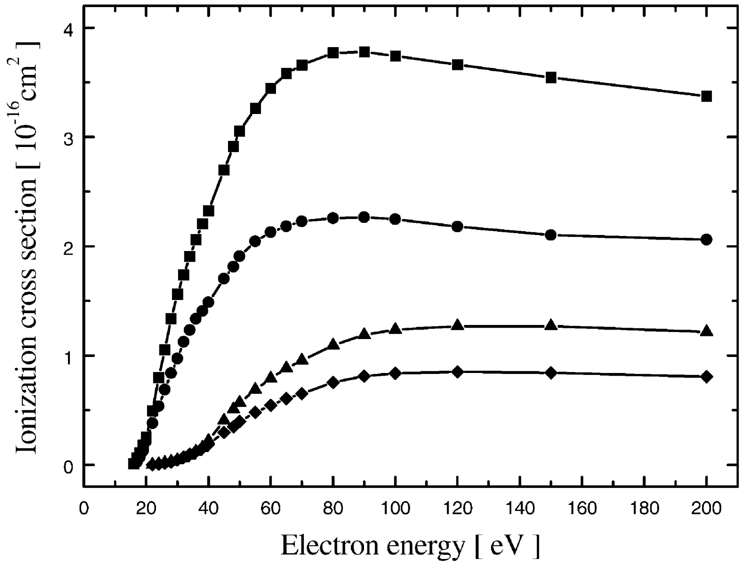

Fig. 2. Absolute partial C_2F_6 ionization cross sections of the fragment ions CF_3^+ (squares), $C_2F_5^+$ (circles), CF^+ (triangles), and CF_2^+ (diamonds) as a function of electron energy.

and CF_3^+. However, our data appear to be consistently somewhat lower in comparison with [6] but one has to consider the different cross section data used for calibration. Calibration of our ion efficiency curves with the cross section of Ar^+ ($2.65 \times 10^{-16}\,cm^2$ at 70 eV) from the crossed-beam measurements of Wetzel et al. [29] used by Jiao et al. [6] would result in an increase by 6%.

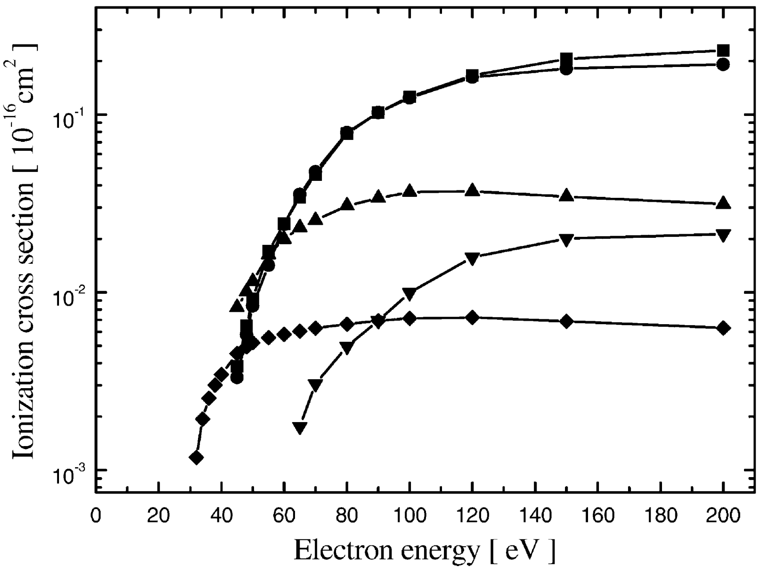

Fig. 3. Absolute partial C_2F_6 ionization cross sections of the fragment ions F^+ (squares), C^+ (circles), C_2F^+ (triangles), C_2^+ (inverted triangles), and $C_2F_4^+$ (diamonds) as a function of electron energy.

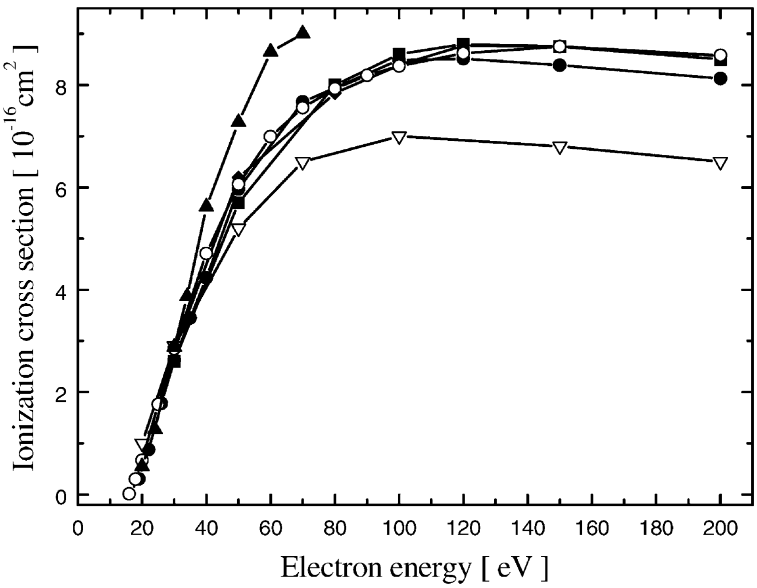

Fig. 4. Absolute total C_2F_6 ionization cross section as a function of electron energy. The present results are shown as the filled circles. The other symbols correspond to the experimental results of [25] (filled diamonds), and [6] (filled triangles) the calculated results of [25] (squares), the calculated results using the MAR [30] (open inverted triangles), and the recommended cross section of [2] (open circles).

Fig. 3 shows our measured partial ionizations cross sections of F^+, C^+, C_2F^+, C_2^+, and $C_2F_4^+$ which are all formed with comparatively small maximum cross sections of $0.2 \times 10^{-16}\,cm^2$ or less. To the best of our knowledge, no other experimental data for these partial cross sections are available in the literature.

On the basis of the nine partial ionization cross sections reported here, we can derive a total (single) ionization cross section for C_2F_6 (also listed in Table 3 as the last column) and compare the result with other measured and calculated total ionization cross sections for this molecule. The result is shown in Fig. 4. Our total C_2F_6 ionization cross section is in excellent agreement with the measured cross section of Nishimura et al. [25], the calculated cross section using the BEB method of Nishimura et al. [25] in conjunction with CAS wave functions, and with the recommended cross section of [2]. The total cross section of [6] exceeds all these values above 35 eV impact energy. The difference rises up to 19% at 70 eV. A calculated C_2F_6 ionization cross section using the semi-empirical Modified Additivity Rule (MAR) of Deutsch et al. [30] lies about 20% below all other cross sections (which is a frequently observed finding when the MAR is applied to halogen-containing complex molecules [30]).

4. Conclusions

We measured the absolute partial electron ionization cross sections for the formation of molecular and atomic fragment ions from C_2F_6 using a TOF-MS. The reliable performance of the apparatus was demonstrated by reproducing the benchmark cross sections for the formation of fragment ions from CF_4. The partial cross sections of C_2F_6 for the formation of the most abundant molecular fragment ions CF_3^+, $C_2F_5^+$, CF^+, and CF_2^+ are determined along with the considerably smaller cross sections for the formation of the ions $C_2F_4^+$, C_2F^+, C_2^+, F^+, and C^+. As in the case of CF_4, no parent ion is formed for C_2F_6, but in contrast to CF_4 no doubly charged fragment ions were observed in the case of C_2F_6.

We note in particular, that absolute ionization cross sections for C_2F_6 have now been measured using several different experimental methods (TOF-MS, Fourier transform mass spectrometer [6], quadrupole mass spectrometer [4], parallel-plate type apparatus [25]) and the results are in good agreement, at least for the larger partial cross sections and for the total cross section. The present results in conjunction with the results of the electron ionization studies of the CF_x ($x = 1$–3) free radicals [31,32] and C_2F_5 radical [28] provide a reliable and comprehensive data base of ionization cross sections for the modeling of the electron impact-induced ion formation in C_2F_6-containing plasmas.

Acknowledgements

The authors thank the DAAD for supporting the stay of ED at the INP. Two of us (P.L., K.B.) would like to acknowledge partial financial support by the Division of Chemical Science, Office of Basic Energy Sciences, Office of Energy Research, US Department of Energy. We are grateful for the technical assistance provided by Ms. U. Haeder.

References

[1] L.G. Christophorou, J.K. Olthoff, M.V.V.S. Rao, J. Phys. Chem. Ref. Data 25 (1996) 1341.
[2] L.G. Christophorou, J.K. Olthoff, J. Phys. Chem. Ref. Data 27 (1998) 1.
[3] L.G. Christophorou, J.K. Olthoff, J. Phys. Chem. Ref. Data 27 (1998) 889.
[4] H.U. Poll, J. Meichsner, Contrib. Plasma Phys. 27 (1987) 5, 359
[5] M. Bibby, G. Carter, Trans. Faraday Soc. 59 (1963) 2455.
[6] C.Q. Jiao, A. Garscadden, P.D. Haaland, Chem. Phys. Lett. 310 (1999) 52.
[7] V. Tarnovsky, A. Levin, K. Becker, R. Basner, M. Schmidt, Int. J. Mass Spectrom. Ion Processes 133 (1994) 175.
[8] R. Basner, M. Schmidt, V. Tarnovsky, A. Levin, K. Becker, J. Chem. Phys. 103 (1995) 211.
[9] R. Basner, M. Schmidt, H. Deutsch, Contrib. Plasma Phys. 35 (1995) 375.
[10] R. Basner, R. Foest, M. Schmidt, F. Sigeneger, P. Kurunczi, K. Becker, H. Deutsch, Int. J. Mass Spectrom. Ion Processes 153 (1996) 65.
[11] R. Basner, M. Schmidt, V. Tarnovsky, K. Becker, H. Deutsch, Int. J. Mass Spectrom. Ion Processes 171 (1997) 83.
[12] R. Basner, R. Foest, M. Schmidt, K. Becker, H. Deutsch, Int. J. Mass Spectrom. 176 (1997) 245.
[13] R. Basner, M. Schmidt, K. Becker, V. Tarnovsky, H. Deutsch, Thin Solid Films 374 (2000) 291.
[14] R. Basner, M. Schmidt, E. Denisov, K. Becker, H. Deutsch, J. Chem. Phys. 114 (2001) 1170.
[15] C. Ma, C.R. Sporleder, R.A. Bonham, Rev. Sci. Instrum. 62 (4) (1991) 909.
[16] H.C. Straub, P. Renault, B.G. Lindsay, K.A. Smith, R.F. Stebbings, Phys. Rev. A 52 (2) (1995) 1115.
[17] C. Ma, M.R. Bruce, R.A. Bonham, Phys. Rev. A 44 (1991) 2921 [Erratum 45 (1992) 6932].
[18] M.R. Bruce, C. Ma, R.A. Bonham, Chem. Phys. Lett. 190 (1992) 285.
[19] M.R. Bruce, R.A. Bonham, Intern. J. Mass Spectrom. Ion Processes 123 (1993) 97.
[20] R.A. Bonham, Jpn. J. Appl. Phys. 33 (1994) 4157.
[21] M.R. Bruce, R.A. Bonham, J. Mol. Structure 352/353 (1995) 235.
[22] K. Stephan, H. Deutsch, T.D. Märk, J. Chem. Phys. 83 (1985) 5712.
[23] H.U. Poll, C. Winkler, D. Margreiter, V. Grill, T.D. Märk, Int. J. Mass Spectrom. Ion Processes 112 (1992) 1.
[24] R. Basner, M. Schmidt, E. Denisov, H. Deutsch, P. Lopata, V. Tarnovsky, K. Becker, in: Proceedings of XXIV ICPIG, Vol. 4, 1999, p. 17.
[25] H. Nishimura, W.M. Huo, M.A. Ali, Y.-K. Kim, J. Chem. Phys. 110 (1999) 3811.
[26] D. Rapp, J. Englander-Golden, Chem. Phys. 43 (1965) 1464.
[27] V.H. Dibeler, R.M. Reese, F.L. Mohler, J. Res. Bureau Standards 57 (1956) 113.
[28] V. Tarnovsky, H. Deutsch, K. Becker, J. Phys. B 32 (1999) L573.
[29] R.C. Wetzel, F.A. Baioochi, T.R. Hayes, R.S. Freund, Phys. Rev. 35 (1987) 559.
[30] H. Deutsch, K. Becker, R. Basner, M. Schmidt, T.D. Märk, J. Phys. Chem. 102 (1998) 8819.
[31] V. Tarnovsky, P. Kurunczi, D. Roghoshnikov, K. Becker, Int. J. Mass Spectrom. Ion Processes 128 (1993) 181.
[32] V. Tarnovsky, K. Becker, J. Chem. Phys. 98 (1993) 7868.